Topological Insulator Surface States and Electrical Transport

This notes are predominately based on:

- J.K. Asbóth, L. Oroszlány and A. Pályi. A Short Course on Topological Insulators "http://arxiv.org/abs/1509.02295" (2015).
- The Quantum Spin Hall Effect: Theory and Experiment, M. König *et al*, J. Phys. Soc. Jpn. **77**, 031007 (2008).
- X-L. Qi and S-C. Zhang, Rev. Mod. Phys. **83**, 1057 (2011).
- G. Tkachov and E.M. Hankiewicz, Phys. Status Solidi B **250**, 215-232 (2013).

and several other papers referenced throughout these sides.

Contents

We would like to be able to construct an effective theory of the edge states of a 2D TI. We shall start for the BHZ model introduced in an earlier lecture

$$H = \begin{bmatrix} h(\mathbf{k}) & 0 \\ 0 & h^*(-\mathbf{k}) \end{bmatrix}$$

in which

$$h(\mathbf{k}) = \mathcal{A}(\sigma_x k_x - \sigma_y k_y) + \mathcal{M}_{\mathbf{k}}\sigma_z + \mathcal{D}\mathbf{k}^2\sigma_0$$
$$\mathcal{M}_{\mathbf{k}} = \mathcal{M} + \mathcal{B}\mathbf{k}^2$$

where σ_i acts in the spin space and $\mathcal{A}$, $\mathcal{B}$, $\mathcal{D}$ and $\mathcal{M}$ are material parameters that depend on the QW geometry and M varying with QW thickness and changing sign at a critical thickness d_c.

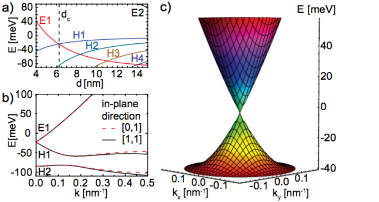

Figure 3 (online color at: www.pss-b.com) Band structure of a $HgTe/Hg_{0.3}Cd_{0.7}Te$ quantum well: (a) electron $E1$, $E2, \ldots$ and heavy-hole $H1$, $H2, \cdots$ subband energies versus well thickness d, (b) in plane dispersion at the critical thickness $d_c \approx 6.3$ nm, and (c) a 3D plot of the Dirac-like low-energy spectrum for $d = d_c$ near the Γ point of the Brillouin zone (adapted from [69]).

- This Hamiltonian is valid near the Γ hugh symmetry point of the BZ.
- We model neglects some terms found via a full $\mathbf{k} \cdot \mathbf{p}$ model. This hamiltonian will capture the physics we are interested in and we will return to consider the missing terms in a later slide.
- using the unitary transform $U = \begin{pmatrix} 0 & \sigma_z \\ -i\sigma_y & 0 \end{pmatrix}$ we can transform the Hamiltonian into the Dirac like form

$$H = \tau_z \boldsymbol{\sigma} \cdot (\mathcal{A}\mathbf{k} + \mathcal{M}_{\mathbf{k}}\mathbf{z}) + \mathcal{D}\mathbf{k}^2 \tau_0 \sigma_0$$

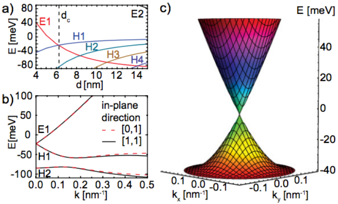

Figure 3 (online color at: www.pss-b.com) Band structure of a HgTe/$Hg_{0.3}Cd_{0.7}Te$ quantum well: (a) electron $E1$, $E2$, ... and heavy-hole $H1$, $H2$, $\cdots$ subband energies versus well thickness d, (b) in plane dispersion at the critical thickness $d_c \approx 6.3$ nm, and (c) a 3D plot of the Dirac-like low-energy spectrum for $d = d_c$ near the Γ point of the Brillouin zone (adapted from [69]).

Edge States of a 2D Topological Insulator

As we consider states near $\Gamma(\mathbf{k} = 0)$, we will omit terms $\propto \mathbf{k}^2$. Now we find, in the position representation, an equation for the four component wave function $\Psi(\mathbf{r})$,

$$[\epsilon\sigma_0 = \tau_z \boldsymbol{\sigma} \cdot (-i\mathcal{A}\nabla + \mathcal{M}\mathbf{z})]\Psi(\mathbf{r}) = 0$$

We now assume our system is confined by a normal band insulator with infinite mass, $M \to \infty$. So we will seek to introduce the boundary conditions

$$\Psi(x, y = 0) = \tau_0 \sigma_x \Psi(x, y = 0)$$

We must note that these boundary are specific to Dirac fermions with a linear spectrum. It ensures vanishing of the normal component of the particle current without putting $\Psi(\mathbf{r})$ to zero at the boundary. Other approaches can be constructed for model with include $\propto \mathbf{k}^2$ terms.

Edge States of a 2D Topological Insulator

We seek solutions in form of the two eigenstates, $\Psi_{k,\pm}(\mathbf{r})$ of diagonal matrix $\tau_z\sigma_0$ propagating along the edge (in the x-direction) and decaying exponentially away from it (in the y-direction),

$$\Psi_{k,+}(\mathbf{r}) = \begin{pmatrix} 1 \\ 0 \end{pmatrix} \otimes \begin{pmatrix} \Psi_{1k+} \\ \Psi_{2k+} \end{pmatrix} e^{ikx-y/\lambda}$$

$$\Psi_{k,-}(\mathbf{r}) = \begin{pmatrix} 0 \\ 1 \end{pmatrix} \otimes \begin{pmatrix} \Psi_{1k-} \\ \Psi_{2k-} \end{pmatrix} e^{ikx-y/\lambda}$$

with a real positive decay length λ. Now using the boundary condition we will find two expressions for λ and ϵ

$$\lambda^{-2} - \frac{\mathcal{M}^2}{\mathcal{A}^2} = k^2 - \frac{\epsilon^2}{\mathcal{A}^2} \qquad \lambda^{-1} + \frac{\mathcal{M}}{\mathcal{A}} = k - \frac{\epsilon}{\tau\mathcal{A}} \qquad \tau = \pm 1$$

The τ means that these equation vanish independently. Solving this gives a gapless linear dispersion and real decay length (for $\mathcal{M} < 0$).

$$\epsilon_{k\tau} = \tau\mathcal{A}k \quad ; \qquad \lambda = -\frac{\mathcal{A}}{\mathcal{M}}$$

Edge States of a 2D Topological Insulator

Therefore we find the edge state wave functions normalised to half-space $0 \le y < \infty$ are given by

$$\Psi_{k,+}(\mathbf{r}) = \begin{pmatrix} 1 \\ 0 \end{pmatrix} \otimes \begin{pmatrix} 1 \\ 1 \end{pmatrix} \sqrt{\frac{|\mathcal{M}|}{\mathcal{A}}} e^{ikx - |\mathcal{M}|y/A}$$
$$\Psi_{k,-}(\mathbf{r}) = \begin{pmatrix} 0 \\ 1 \end{pmatrix} \otimes \begin{pmatrix} 1 \\ 1 \end{pmatrix} \sqrt{\frac{|\mathcal{M}|}{\mathcal{A}}} e^{ikx - |\mathcal{M}|y/A}$$

A key feature is that they are orthogonal eigenstates of the helicity operator $\Sigma = \tau_z \sigma_x$

$$\Sigma \Psi_{k,\tau}(\mathbf{r}) = \tau \Psi_{k,\tau}(\mathbf{r}), \quad \tau = \pm 1$$

The helicity Σ is defined as the projection of the vector $\Sigma = \tau_z \sigma$ on the direction of the edge-state momentum $\mathbf{k}||x$. These helical states are Kramers pairs and are related by time reversal operator $\mathcal{T} = i\tau_y \sigma_x \mathcal{C}$,

$$\Psi_{k,+} = \mathcal{T}\Psi_{-k,-} \quad \Psi_{-k,-} = -\mathcal{T}\Psi_{k,+}$$

Edge States of a 2D Topological Insulator

In a previous slide we noted that we had neglected some small terms. Their inclusion causes the edge state spectrum to become gapped - *a big difference!*. This arises due to finite size effects as the two edges may hybridise with each other. This opens a gap in the edge states of magnitude

$$\Delta \simeq \frac{4|\mathcal{A}\mathcal{B}_+\mathcal{B}_-\mathcal{M}|}{\sqrt{\mathcal{B}^3(\mathcal{A}^2\mathcal{B} - 4\mathcal{B}_+\mathcal{B}_-\mathcal{M})}} e^{-\lambda L}$$

with $\mathcal{B}_\pm = \mathcal{B} \pm \mathcal{D}$. For $L = 1000$nm we find $\Delta = 1.4 \times 10^{-7}$meV, but for $L = 200$nm we will find $\Delta = 0.45$meV which is in principle observable.

Phys. Rev. Lett. 101, 246807 (2008)

Edge States of a 2D Topological Insulator

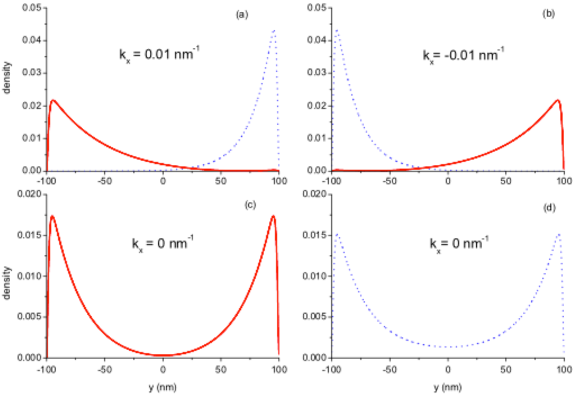

FIG. 2 (color online). The density distribution of the two edge states $\Psi_{\uparrow\pm}(k_x, y)$ for $L = 200$ nm. (a) The solid line corresponds to $|\Psi_{\uparrow+}(k_x, y)|^2$, and the dotted line to $|\Psi_{\uparrow+}(-k_x, y)|^2$ at $k_x = 0.01$ nm^{-1}; (b) The solid line corresponds to $|\Psi_{\uparrow-}(k_x, y)|^2$, and the dotted line to $|\Psi_{\uparrow-}(-k_x, y)|^2$ at $k_x = -0.01$ nm^{-1}; (c) and (d) for $k_x = 0$ nm^{-1}.

Phys. Rev. Lett. 101, 246807 (2008)

Edge States - Mass Term

We can also write an effective Hamiltonian for *only* the edge states, this Hamiltonian is known as the helical Luttinger Liquid. The Luttinger liquid theory allows for the description of interacting 1D fermonic system, and will only be discussed here very briefly as it's not the focus of this course. The Hamiltonian after linearising around the fermi energy is given by

$$H_0 = v_F \int dx \big[\psi^\dagger_{R,\uparrow}(x) i\partial_x \psi_{R,\uparrow}(x) - \psi^\dagger_{L,\downarrow}(x) i\partial_x \psi_{L,\downarrow}(x) \big]$$

we can try and introduce a "mass" term which will gap the spectrum

$$H_{\text{mass}} = \int dx m \big[\psi^\dagger_{R,\uparrow}(x) \psi_{L,\downarrow}(x) + h.c. \big]$$

However, the time-reversal symmetry of the electron system is expressed as

$$\mathcal{T}^{-1} \psi_{R,\uparrow}(x) \mathcal{T} = \psi_{L,\downarrow} \quad \mathcal{T}^{-1} \psi_{L,\downarrow}(x) \mathcal{T} = -\psi_{R,\uparrow}$$

which will give rise to

$$\mathcal{T}^{-1} H_{\text{mass}} \mathcal{T} = -H_{\text{mass}}$$

Edge States - Interactions

Imagine that at $t = 0$, n right movers are excited, and consider whether they can be scattered back to n left movers by a random potential. Specifically, assume that the final state of n left movers $|\psi\rangle$ is the $\mathcal{T}$ conjugates of the right-moving initial state $|\phi\rangle$ The matrix element for H' to connect these states is

$$\langle\psi|H'|\phi\rangle = \langle\mathcal{T}\phi|H'|\phi\rangle = \langle\mathcal{T}|H'|\mathcal{T}^2\phi\rangle$$
$$(-1)^n\langle\mathcal{T}\phi|H'|\phi\rangle = (-1)^n\langle\psi|H'|\phi\rangle$$

For n odd, this process is forbidden because the matrix element has to be zero. However for n even inter branch scattering can happen, for example the only 2 particle interaction allowed are

$$H_{\text{fw}} = g\int dx\psi^{\dagger}_{R,\uparrow}(x)\psi_{R,\uparrow}(x)\psi^{\dagger}_{L,\downarrow}(x)\psi_{L,\downarrow}(x)$$

$$H_{\text{um}} = g_u\int dx e^{-i4k_F x}\psi^{\dagger}_{R,\uparrow}(x)\psi^{\dagger}_{R,\uparrow}(x+a)\psi_{L,\downarrow}(x+a)\psi_{L,\downarrow}(x) + h.c.$$

Edge States - No Go Theorems

- Kramers Pair states must reform with each other as k goes to 0, π , $-\pi$ requiring crossing Fermi level 4n times. - But is allows single particle scattering!
- But we realise they merge in bulk states as some large k and can match at $k = \pm\pi$ with edge states for other edge.
- therefore the helical edges states can only be stable as a holographic theory on a 2D theory.

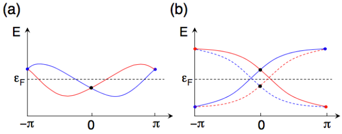

Figure 4: (a) The energy dispersion of a one-dimensional time-reversal invariant system. Kramer's degeneracy is required at $k = 0$ and $k = \pi$, so that the energy spectrum always crosses the Fermi level ϵ_F $4n$ times. (b) The energy dispersion of the helical edge states on one boundary of the QSH system (solid lines). At $k = 0$ the edge states are Kramers' partners of each other, while at $k = \pi$ they merge to the bulk and pair with the edge states of the other boundary (dash lines). In both (a) and (b), red and blue lines form Kramers' partners of each other.

Edge States - Transport theory

We use the Landauer-Bütikker formalism. Here the current through contact I_i through the multi terminal device with voltages V_i is

$$I_i = \frac{e^2}{h}\sum_{j=1}^{N}(T_{ji}V_i - T_{ij}V_j)$$

and T_{ij} is the transmission probability for contact i to contact j. For quantum spin hall edge states with helical edge channels we use the only non vanishing transmission probabilities are $T_{i+1,i} = T_{i,i+1} = 1$.

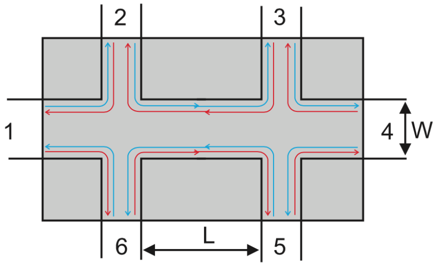

Edge States - Transport theory

Considering the example of current leads on electrodes 1 and 4, and voltage leads on electrodes 2, 3, 5 and 6, one finds that
$I_1 = -I_4 \equiv I_{14}$,
$V_2 - V_3 = (h/2e^2)I_{14}$, and
$V_1 - V_4 = (3h/e^2)I_{14}$, giving a four-terminal resistance of $R_{14,23} = h/2e^2$ and a two-terminal resistance of $R_{12,14} = 3h/2e^2$.

- So we see a *non-local* signal in the resistance

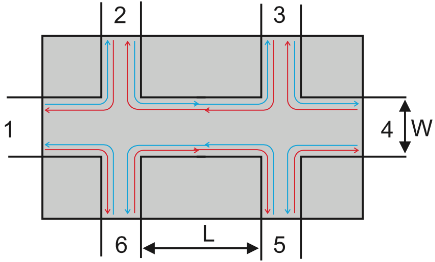

Edge States - Longitudinal Resistance

Fig. 4. The longitudinal four-terminal resistance, $R_{14,23}$, of various normal ($d = 5.5$ nm) (I) and inverted ($d = 7.3$ nm) (II, III, and IV) QW structures as a function of the gate voltage measured for $B = 0$ T at $T = 30$ mK. The device sizes are (20.0×13.3) μm^2 for devices I and II, (1.0×1.0) μm^2 for device III, and (1.0×0.5) μm^2 for device IV. The inset shows $R_{14,23}(V_g)$ of two samples from the same wafer, having the same device size (III) at 30 mK (green) and 1.8 K (black) on a linear scale.

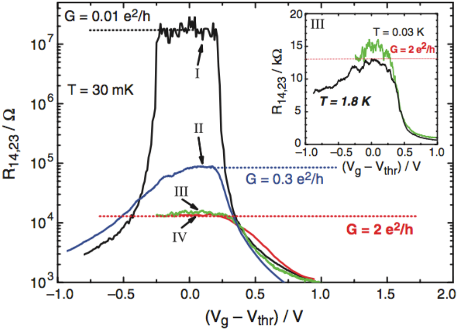

Science 318, 766 (2007)

Edge States of a 2D Topological Insulator

We would also want to explore the effect of a external magnetic field on the edge states, we can introduce the effect of a B-field with the substitution $\mathbf{k} \to (\mathbf{k} + e\mathbf{A})$ and choose the symmetric gauge $\mathbf{A} = B/2(-y, x)$, this allows us to define the new operators

$$\pi^{+} = \hbar\left(k_{+} + \frac{ieB}{2\hbar}z\right) \quad , \quad \pi^{-} = \hbar\left(k_{-} - \frac{ieB}{2\hbar}z^{*}\right)$$

where $k_{\pm} = k_x \pm ik_y$ and $z = x + iy$. These mechanical momenta have the commutation relation $[\pi_{+}, \pi_{-}] = -2\hbar^2/l_B^2$ with the magnetic length $l_B = (\hbar/eB)^{1/2}$. Finally we can use these to define the lowering and raising operators

$$a = \frac{l_B}{\hbar}\pi^{-} \quad , \quad a^{\dagger} = \frac{l_B}{\hbar}\pi^{+}$$

and $[a, a^{\dagger}] = 1$. How the subblocks of the BHZ Hamiltonian can be written as $h(a, a^{\dagger})$.

Edge States of a 2D Topological Insulator

Solve the BHZ with these magnetic fields included we will find the energy spectrum

$$E_\alpha = -\omega_0^D n - \alpha\frac{\omega_0^B}{2} \pm \sqrt{\frac{2\mathcal{A}^2 n}{l_B^2} + (\mathcal{M} - n\omega_0^B - \frac{\alpha}{2}\omega_0^D)^2}$$

where $\omega_0^B = 2\mathcal{B}/l_B^2$, $\omega_0^D = 2\mathcal{D}/l_B^2$ and $\alpha = \pm 1$.

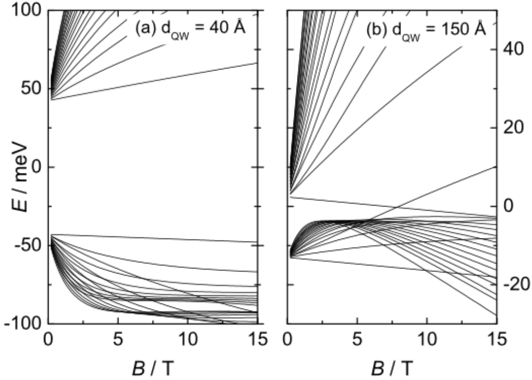

Edge States of a 2D Topological Insulator

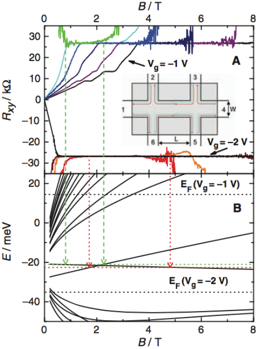

Fig. 1. (**A**) Hall resistance, R_{xy}, of a ($L \times W$) = (600 × 200) μm^2 QW structure with 6.5-nm well width for different carrier concentrations obtained for gate voltages V_g of −1.0 V (black), −1.1 V (purple), −1.2 V (navy), −1.3 V (blue), −1.35 V (cyan), −1.4 V (green), −1.7 V (red), −1.8 V (orange), −1.9 V (brown), and −2.0 V (black, lower curve). For decreasing V_g, the n-type carrier concentration decreases and a transition to a p-type conductor is observed, passing through an insulating regime between −1.4 and −1.9 V at B = 0 T. The inset shows a schematic sample layout with ohmic contacts labeled 1 to 6. The gray shaded region indicates the top gate electrode and defines the part of the sample where the carrier concentration and type can be changed. Red and blue arrows indicate the counterpropagating spin-polarized edge channels of the QSH effect. (**B**) The Landau-level fan chart of a 6.5-nm QW obtained from an eight-band **k·p** calculation. Black dashed lines indicate the energetic position of the Fermi energy, E_F, for V_g = −1.0 and −2.0 V. Red and green dashed lines correspond to the position of the Fermi energies of the red and green Hall resistance traces of (A). The Landau-level crossing points are marked by arrows of the same color.

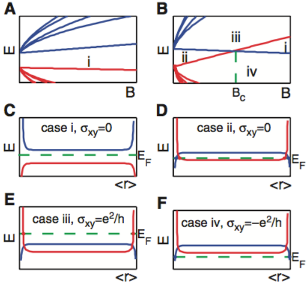

Science 318, 766 (2007)

Edge States - Weak Anti-Localisation

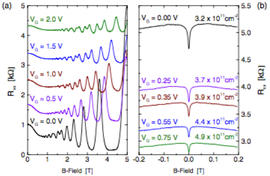

- FIG. 1 (color online). Magnetoresistance ($d = 7$ nm), $R_{xx}(B)$, of (a) a macroscopic Hall bar with $30 \times 10\ \mu\text{m}^2$ at $T = 4.2$ K and (b) 40 parallel wires with $50 \times 0.37\ \mu\text{m}^2$ area for different gate voltages V_G at $T = 1.8$ K. For clarity, the traces of Fig. 1(a) are displayed with a constant offset of 1 kΩ. The corresponding measured carrier densities are $n = 3.2$, 4.3, 5.4, 6.7, and $7.9 \times 10^{11}\ \text{cm}^{-2}$ for the indicated gate voltage. For the multiple wire sample of Fig. 1(b), the carrier densities are indicated in the figure.

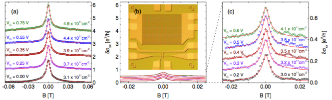

- FIG. 2 (color online). WAL contribution to the magnetoconductivity, $\delta\sigma_{xx}(B)$, for wires of the 7 nm (inverted) QW, (a), and of the 5 nm (normal) QW, (b) and (c) at different gate voltages V_g at $T = 1.8$ K. The thin (red) lines are fits based on Eqs. (1)–(3). Subsequent curves are shifted by e^2/h in (a) and by $0.1e^2/h$ in (b) and (c) for clarity. The inset of (b) shows the mesa structure of measured samples.

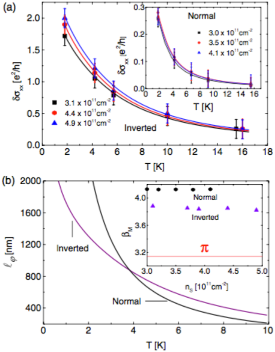

FIG. 3 (color online). (a) Temperature dependence of the conductivity $\delta\sigma_{xx}(T)$ for wires of the 7 (inverted) QW and 5 nm (normal) QW (inset) at different gate voltages. The solid lines are fits based on Eqs. (1)–(3). (b) Extracted dephasing length for wires of the inverted and normal QW at $V_g = 0$. Inset: Extracted Berry phase, β_M, versus carrier density n_s for inverted and normal samples.

Phys. Rev. Lett. **112**, 146803 (2014)